



# Exploring effects of novel chemical modification of biochar on soil water retention and crack suppression: towards commercialization of production of biochar for soil remediation

Yongxue An<sup>1</sup> · Jinling Lu<sup>1</sup> · Renjie Niu<sup>1</sup> · Manqi Li<sup>1</sup> · Xiangnan Zhao<sup>1</sup> · Xilong Huang<sup>1</sup> · He Huang<sup>1</sup> · Ankit Garg<sup>1</sup> · Askar Zhussupbekov<sup>2</sup>

Received: 23 August 2021 / Revised: 25 October 2021 / Accepted: 1 November 2021 / Published online: 19 November 2021  
© The Author(s), under exclusive licence to Springer-Verlag GmbH Germany, part of Springer Nature 2021

## Abstract

Recently, incentives have been provided in developed countries for promoting commercialization of biochar production for usage in construction industry. One of the main reasons for such incentives is the carbon sequestration capacity of biochar, which can be highly useful for countries to meet their goals of carbon emission reduction by 2030. In this regard, chemical modification of biochars has also been done to enhance their surface area and functionality, which is useful for adsorption of pollutants. However, rarely any studies are conducted to explore the effect of chemical treatment of biochar on soil cracking and water retention. The major objective of this study is to explore the crack and water retention properties of chemically modified biochar amended soil. Pig manure biochar (PMB) and peach shell biochar (PSB) with contrasting compositions were modified with  $H_3PO_4$  and KOH. Soils were mixed with modified biochars at four dosages (0, 2, 5, and 8%). Crack intensity factor (CIF) and moisture content were measured during drying-wetting cycles. Results showed that  $H_3PO_4$ -modified biochar has been found to have a higher impact on water retention as compared to KOH-modified biochar. KOH modification instead tends to reduce hydrophilic functional groups on surface of biochar. Pig manure biochar appears to have a higher crack suppression capacity than even functional biochars. In most cases, 5–8% biochar dosage is generally found to be an optimal range for reducing cracks and improving water retention. Based on the given testing conditions, the effect of chemical modification of biochar on cracking appears to be inconclusive. It should be noted that the results in this study are based on a given testing conditions and generalization requires further studies on different types of soils.

**Keywords** Biochar · Chemical modification · Crack intensity factor · Water retention

## List of notations

$\omega$  Water content (%)

$m_0$  Weight of dry soil (g)

$m_1$  Weight of sample (g)

$m_2$  Initial weight of sample (g)

$\mu$  Crack intensity factor (%)

$p'$  Number of the pixels of crack (dimensionless)

$p$  Total pixels number of the dish (dimensionless)

✉ Ankit Garg  
ankit@stu.edu.cn

Yongxue An  
19yxan@stu.edu.cn

Jinling Lu  
19jllu@stu.edu.cn

Renjie Niu  
18rjniu@stu.edu.cn

Manqi Li  
18mqli3@stu.edu.cn

Xiangnan Zhao  
18xnzhao@stu.edu.cn

Xilong Huang  
18xlhuang1@stu.edu.cn

He Huang  
18hhuang2@stu.edu.cn

Askar Zhussupbekov  
astana-geostroi@mail.ru

<sup>1</sup> Guangdong Engineering Center for Structure Safety and Health Monitoring, Department of Civil and Environmental Engineering, Shantou University, Guangdong 515063, China

<sup>2</sup> L.N. Gumilyov Eurasian National University, Nur-Sultan 010000, Kazakhstan

## 1 Introduction

Crack and water retention capacity of soil is significant in influencing water balancing in green infrastructure (i.e., green roofs and bio-filters). Improving water retention and suppression of cracking can help in holding more water at near surface of soil, which is important for vegetation growth. Soil additives such as fiber [1], microorganism [2, 3], and silica powder [4] have been adopted to suppress cracking. Liu et al. [5] have also reported the effects of wetting–drying cycles on cracking and water retention of untreated soil and biochar-modified soil [5–7]. However, natural fibers are vulnerable to degradation under influence of microbial activity in long term. In contrast, biochar is a relatively stable carbon, whose half-life period is usually more than 100 years. Biochar has been widely used in improving soil fertility, removing heavy metal ions in water, repairing polluted soil, and reducing landfill gas emissions. It is generally produced at high temperature (above 350 °C) [8]. The characteristics of biochar such as high affinity for water, pore structure, and surface functional groups can improve the infiltration rate, hydraulic conductivity, and water holding capacity of biochar-amended soil [9–12].

It should be noted that half-life of biochar falls well within design period of geotechnical infrastructure (i.e., 30 years). Therefore, it is more appropriate to consider the usage of biochar as compared to degradable fibers in cover material of geotechnical infrastructure. In recent years, chemical treatment of biomass provides a new direction for soil improvement. Chemical-treated natural fibers are likely to have better tensile properties [13]. Use of functional biochars (i.e., chemically treated) is becoming more popular owing to its enhanced specific surface area and functional groups. It was previously studied that the surface area of biochar was increased with an increase in temperature and pH [14]. Chemical modification is a commonly adopted technique for improving physiochemical properties of biochar [15]. The physical and chemical properties of modified biochar depend on the type of raw material, pyrolysis process, pyrolysis temperature, modification method, and modification reagent. The properties of biochar are determined by its molecular structure (porosity and surface area) [16]. The pore structure and surface area are greatly enhanced due to modification of biochar with KOH (denoted as K). Similarly, modification by  $H_3PO_4$  (denoted as P) enhances specific surface area, which is beneficial to the adsorption of water [17, 18]. Biochar has been recognized as renewable, low-cost, and sustainable material [19, 20]. Modified biochar has a significant influence on wastewater treatment [21, 22], adsorption of harmful substances [23–25], and treatment of eutrophic water quality [26]. On the contrary, as far as authors are aware, there are rarely any studies that investigate the effect of chemically modified biochar on soil water retention and cracking. Such

understanding may further motivate commercial production of biochar for its usage in green infrastructure.

Therefore, the main objective of this study is to explore the cracking and water retention properties of soil amended with different functional biochars under drying-wetting cycles. Two types of treatment, i.e., acid ( $H_3PO_4$ ) and base (i.e., KOH) were adopted for modification of biochars derived from peach shell (i.e., plant waste) and pig manure (i.e., animal waste). Hence, four new types of modified biochar were formed, namely, alkaline modified pig manure biochar (KPMB), acid-modified pig manure biochar (PPMB), alkaline-modified peach shell biochar (KPSB), and acid-modified peach shell biochar (PPSB). These four types of biochar were then mixed with relatively loose soil (i.e., compaction of 70%) at amendment rates of 0%, 2%, 5%, and 8% by weight. SEM, BET, FTIR, and XRD were carried out for micro-structural characterization, which is useful for interpretation of cracking and water retention properties. The crack strength factor (CIF) was calculated using image processing technology to quantitatively analyze the cracking.

## 2 Materials and methods

### 2.1 Materials

Analytical pure chemical reagents (KOH and  $H_3PO_4$ ) were used to modify peach shell biochar and pig manure biochar in this research. Phosphoric acid and potassium hydroxide are very common and readily available in China. The materials of biochar in this study are recovered from locally available waste (pig manure, peach shell, etc.). Such feedstock is inexpensive, abundant, and easily available. Before modification, peach shell and pig manure biochar were washed several times with deionized water and then dried in the oven for 24 h. The biochars were sieved to maintain their particles between 2.36 and 4.75 mm.

Chemical modifications are typically done by soaking in solutions at a certain ratio [15]. Impregnation ratios of pure  $H_3PO_4$  to dried biochar (g/g) ranging from 0.8:1 to 4:1 were investigated to obtain high surface-specific area [27]. It is also understood that the mass ratio of KOH to carbon is preferably between 2.5 and 3 [28]. The procedure of preparation of biochar is shown in Fig. 1a. First, 6.0 g each of peach shell biochar and pig manure biochar were kept in marked centrifuge tubes respectively. A weight of 2.0 g KOH and 20 mL deionized water was added to KOH-modified tubes with 3:1 mass ratio of KOH to biochar [28]. An amount of 20 mL (i.e., 47.5% wt.)  $H_3PO_4$  solution was added to phosphoric acid-modified tubes [17]. Then, all the tubes were fully shaken at room temperature for 24 h by keeping them in an oscillator. Biochar was removed from tubes and dried at 80 °C for 24 h. The impregnated biochar was placed in a separate square ceramic crucible and covered with a lid. Crucibles

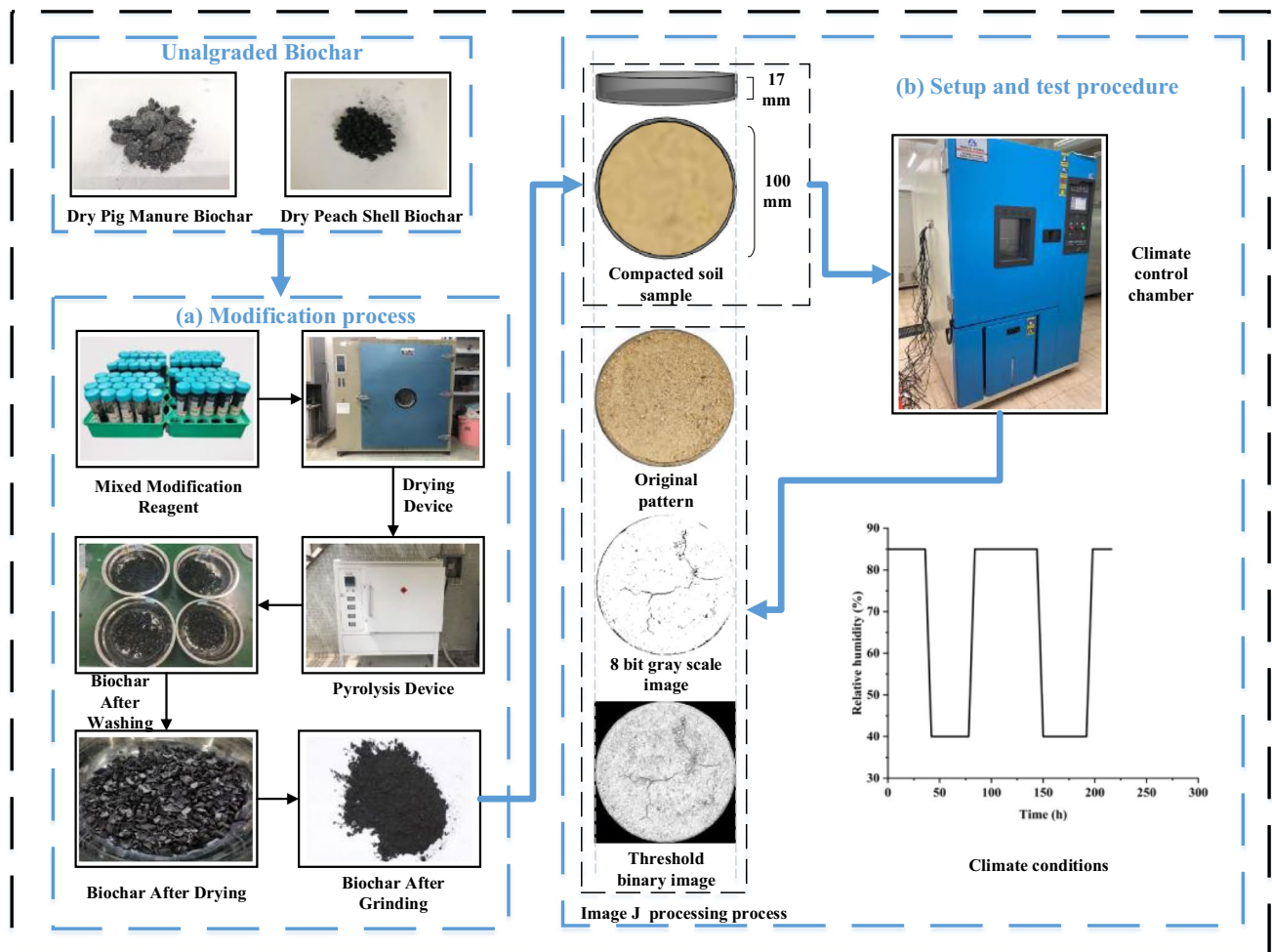


**Fig. 1** Overview of **a** biochar modification experiment and **b** drying-wetting cycle experiment

containing biochar were subjected to 700 °C in a muffle furnace containing nitrogen. A heating rate of 10 °C/min for 2 h was maintained [17]. After cooling down the crucibles at room temperature, the modified biochar was obtained. In order to avoid the adverse effects of modified biochar on the environment, all modified biochars were washed with deionized water repeatedly until the pH of eluent reached stable. Biochar was then dried in the oven to remove any moisture. Finally, the treated biochar was grounded to powder with grinder (AZL-2500C, China) passing through a 0.28 mm sieve (60 mesh) for further usage in experiments.

## 2.2 Modified biochar characterization

In order to understand the mechanism of modification, different techniques were used to characterize pristine and modified biochar. Characterizing the microstructure and surface morphology of biochar was carried out using scanning electron microscopy (SEM; JSM-720, Japan; shown in Fig. 2). Fourier transform infrared (FTIR) spectra were utilized to

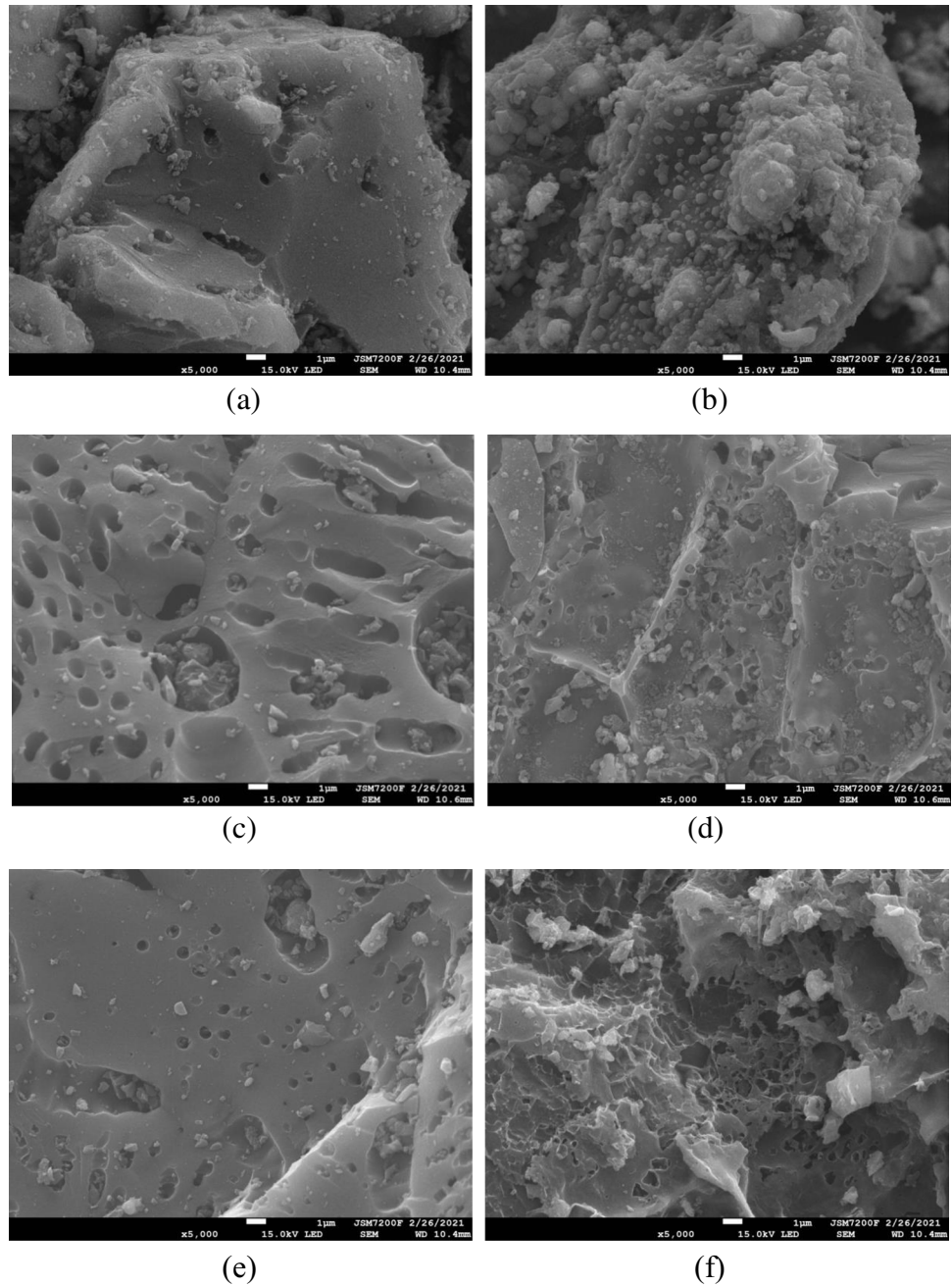
observe functional groups of biochar (FTIR, Nicolette iS50, Thermo Fisher Scientific, Waltham, MA, USA; shown in Fig. 3). Brunauer–Emmett–Teller (BET) (Autosorb-1C, Quanta chrome) method was adopted to measure specific surface area, pore size, and pore volume (refer to Figs. 4 and 5). X-ray diffraction (XRD, D8 Advance, Bruker AXS GmbH, Karlsruhe, Germany) analysis was conducted to identify the surface organic groups of biochar (shown in Fig. 6).

## 2.3 Drying-wetting cycles of modified biochar amended soils

### 2.3.1 Test plan

In this study, soil was collected from a mountain located near Shantou University, Guangdong Province, China. Soil was classified as Clayey Sand (CS) based on United Soil Classification System (USCS; ASTM D2487-17 2017) [29]. Basic geotechnical properties of soil were defined using guidelines prescribed in ASTM standard [23]. Liquid limit (LL) and

**Fig. 2** SEM images of **a** PSB, **b** PMB, **c** KPSB, **d** KPMB, **e** PPSB, and **f** PPMB materials at a magnification of 5000



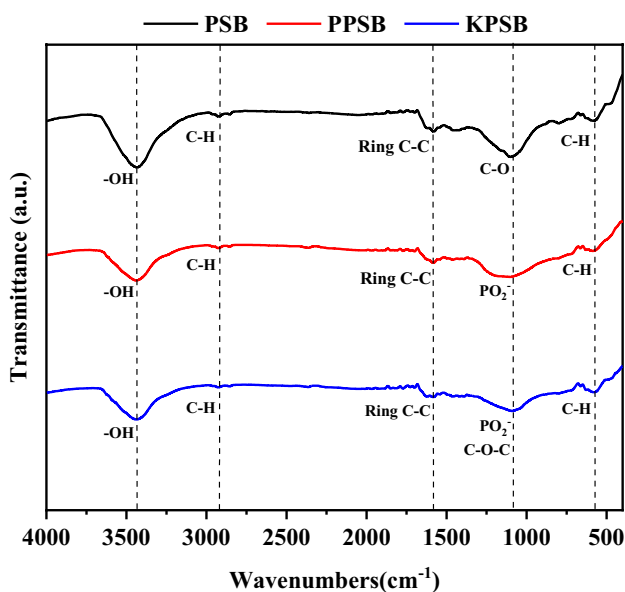
plastic limit (PL) of the soil were obtained as 28.85% and 21.56%, respectively. The maximum dry density (MDD) and optimum moisture content (OMC) of the soil were found to be 1.84 g/cc and 13.6%, respectively.

The soil was sieved through a 0.28-mm sieve and then dried for 24 h in the oven. Four kinds of biochar were mixed with prepared soil in 4 different dosages (0, 2%, 5%, and 8% of soil by weight). The added mass of dry soil was determined by the volume of the glass dishes at MDD. A degree of compaction of 70% is adopted as it corresponds to packing of substrates in agriculture and green infrastructure [30]. Future studies need to be conducted to analyze the impact of degree

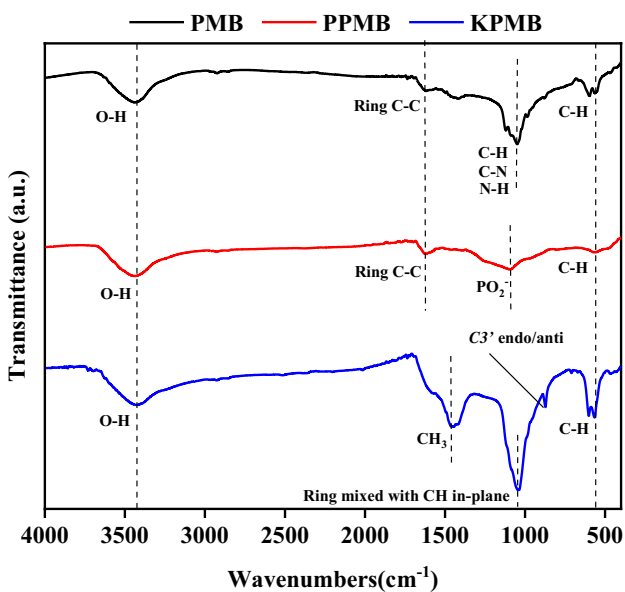
of compaction on water retention and crack desiccation for functional biochar-soil mix. In total, 19 glass-petri dishes (diameter: 108 mm; height: 17 mm) were used for preparing biochar amended soil samples including the control ones at the above-mentioned compaction rate. The detailed experiment plan of this study is summarized in Table 1.

### 2.3.2 Test procedure

The prepared soil specimens were subjected to two drying-wetting cycles (refer to Fig. 1b) for about 216 h. Drying-wetting cycles were induced in a climate control chamber.



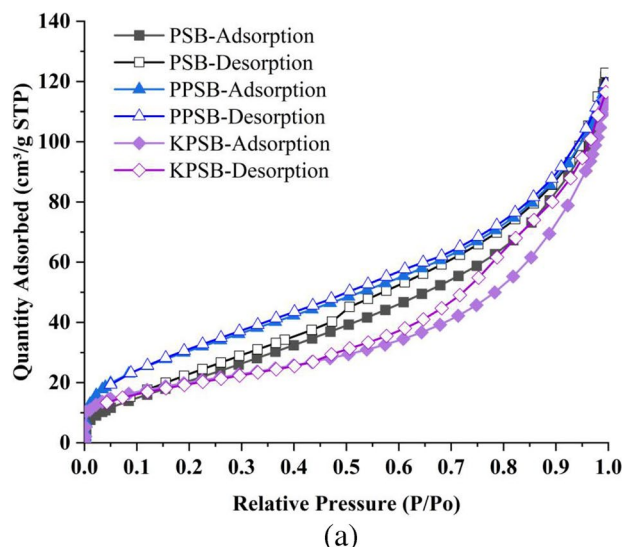
(a)



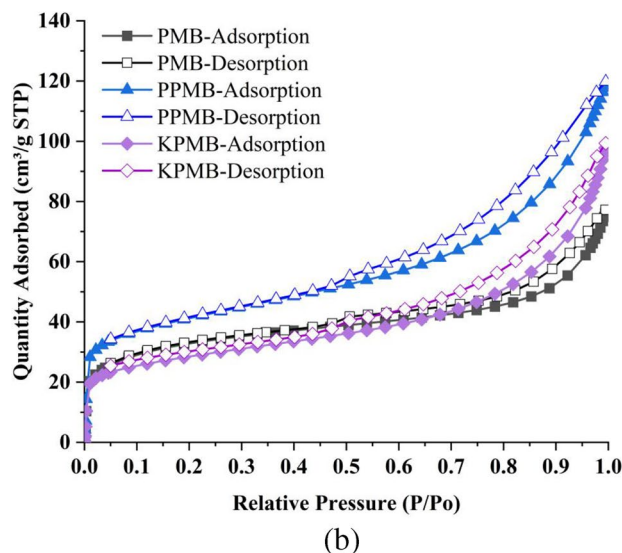
(b)

Fig. 3 FTIR response of a PSB, KPSB, PPSB and b PMB, KPMB, PPMB used in the study

The drying-wetting cycle procedure was based on previous studies on desiccation cracking of soil [31–33]. The drying-wetting experiments consisted of two phases: the dehydration phase and the recovery phase. At the beginning of drying-wetting cycles, samples of biochar amended soils were saturated with deionized water in general atmospheric condition. During the dehydration phase, all specimens were placed in climate control chamber. Relative humidity of 40% was maintained to induce drying. Temperature was



(a)



(b)

Fig. 4 Comparison of N<sub>2</sub> adsorption–desorption isotherms of a PSB, KPSB, PPSB and b PMB, KPMB, PPMB

kept nearly constant at 35 °C. Changes in weight of petri dishes were observed with time. Drying phase continued till negligible change in weight of petri dish was observed. For the recovery phase, 5 mL of deionized water was added in each specimen every 3 h until the soil gets saturated. This was done at constant temperature of 35 °C and humidity of 85% [31]. The weight of samples was measured every 6 h for water content measurement. The gravimetric water content was obtained using oven drying method.

In this study, a high-resolution camera (MER-132-43U3M/C, China) was utilized to capture images of samples for observing the propagation of cracks with 8-bit depth in RGB every 6 h. Images were converted to grey form and dealt with noise removal based on recommendation from

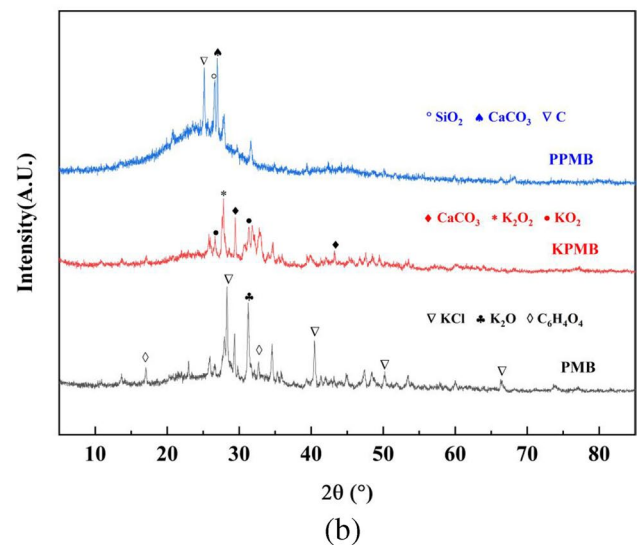
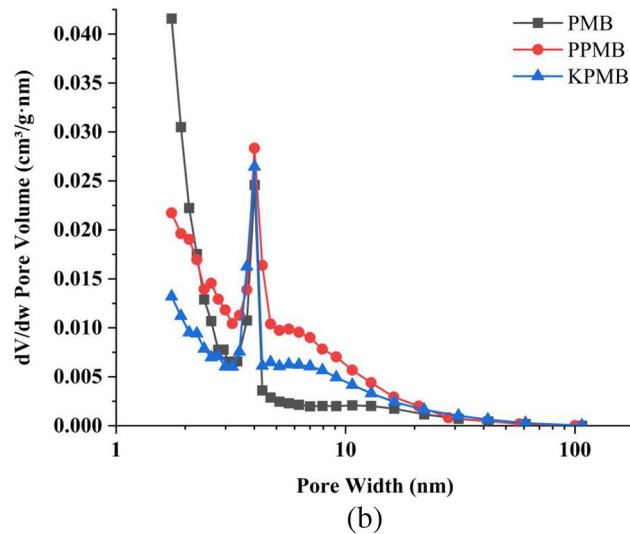
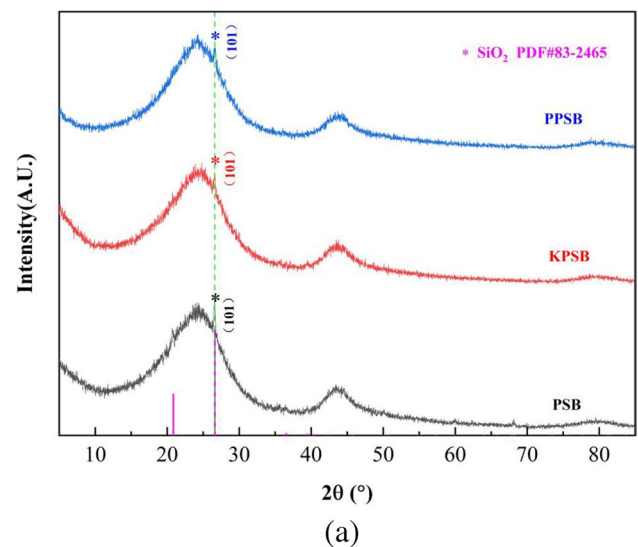
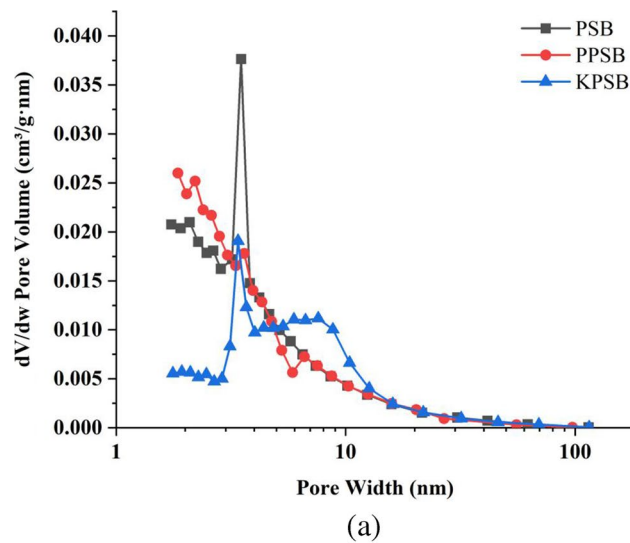


**Fig. 5** Comparison of pore size distribution isotherms of **a** PSB, KPSB, PPSB and **b** PMB, KPMB, PPMB

**Fig. 6** X-ray diffraction of **a** PSB, KPSB, PPSB and **b** PMB, KPMB, PPMB

previous studies [34, 35]. Figure 1b describes the steps for crack measurements. Based on the procession of image using the related application (Image J), the crack intensity was determined in form of crack intensity factor (CIF), which was calculated by the pixels count as suggested in literature [31].

### 3 Results and discussion

#### 3.1 Characteristics of chemically modified biochar

Figure 2 shows the scanning electron microscope images of PSB, PMB, KPSB, KPMB, PPSB, and PPMB. The surface of PSB is smooth with smaller voids (refer to Fig. 2a). After modification with phosphoric acid, more

macro-pores appear to be formed (refer to Fig. 2c). After modification by KOH, the number of pores on the surface of biochar appears to increase along with gradual formation of pore (refer to Fig. 2e). Figure 2b shows that there are many particle projections on the surface of PMB. After the modification of phosphoric acid and potassium hydroxide, the porous structure has undergone significant variation (refer to Fig. 2d, f). The formation of microporous structure of biochar attaches great importance on soil water retention and adsorption capacity [36]. The porosity parameters of all kinds of biochar are summarized in Table 2. The specific surfaces of PPSB and PPMB are 38.30% and 25.89%, respectively higher than those of their corresponding untreated biochars. The average pore sizes of biochar for KPSB and KPMB are 37.58% and 20.94%,

**Table 1** Test program

Materials	Soil/biochar type	Percentage	Sample ID
Soil	Clayey sand	0%	BS
Biochar	Peach shell biochar	2%	PSB-2
		5%	PSB-5
		8%	PSB-8
	KOH-modified peach shell biochar		K-PSB-2
			K-PSB-5
			K-PSB-8
	H <sub>3</sub> PO <sub>4</sub> -modified peach shell biochar		P-PSB-2
			P-PSB-5
			P-PSB-8
	Pig manure biochar		PMB-2
			PMB-5
			PMB-8
KOH-modified pig manure biochar		K-PMB-2	
		K-PMB-5	
		K-PMB-8	
H <sub>3</sub> PO <sub>4</sub> -modified pig manure biochar		P-PMB-2	
		P-PMB-5	
		P-PMB-8	

respectively larger than those of untreated biochars. The surface area obtained using BET method is found to be highest for acid-treated pig manure biochar (i.e., PPMB) followed by PPSB, which is slightly higher than PMB.

Figure 3 shows the FTIR spectrum of six biochar samples. The specific functional groups of peach shell types

of biochar are summarized in Table 3. The spectra of PSB, PPSB, and KPSB presented similar wavenumber, and main bands occurred at 581 cm<sup>-1</sup> (C-H), 1580 cm<sup>-1</sup> (ring C-C), 2923 cm<sup>-1</sup> (C-H), and 3440 cm<sup>-1</sup> (-OH) [37, 38]. The peak appeared at 1099 cm<sup>-1</sup> and had a significant change. The presence of the amino phosphonic acid functional group indicated that a reaction happened between H<sub>3</sub>PO<sub>4</sub> and the carbonaceous components in biochar. The specific functional groups of pig manure types of biochar are summarized in Table 4. Compared with PMB, the intensities of PPMB increased near the peak of 1620 cm<sup>-1</sup>, which indicates formation of additional aromatic compounds. The modification of H<sub>3</sub>PO<sub>4</sub> caused the disappearance of C-N bond and N-H bond. It could be attributed to the volatile NH<sub>3</sub> and the decomposition of nitro and nitrate groups by oxidation during the H<sub>3</sub>PO<sub>4</sub> modification [39]. After KOH modification, ring C-C stretch of phenyl disappeared due to high temperature. Asymmetric CH<sub>3</sub> bending of the methyl groups of proteins indicates the formation of olefin compounds.

Figure 4 shows the N<sub>2</sub> adsorption-desorption isotherms for all samples. As per classification of IUPAC [40], all the adsorption-desorption isotherms are IV type and follow H<sub>4</sub> hysteresis loop. KPSB and KPMB have wider hysteresis loops, indicating that they contain more mesopores. Under the same relative pressure, the adsorption capacity of PPSB and PPMB is larger, indicating better adsorption performance. This is

**Table 2** Porosity parameters of PSB, PMB, PPMB, PPSB, KPMB, and KPSB

Species of biochar	BET surface area (m <sup>2</sup> /g)	Increasing ratio	Desorption cumulative volume of pores (cm <sup>3</sup> /g)	Increasing ratio	Desorption average pore width (4 V/A) (nm)	Increasing ratio	Median pore width (nm)	Increasing ratio
PSB	83.0263	0	0.183181	0	6.3123	0	1.1753	0
KPSB	71.5539	- 13.82%	0.177547	- 3.08%	8.6846	+ 37.58%	1.0313	- 12.25%
PPSB	114.8217	+ 38.30%	0.168520	- 8.00%	6.1255	- 2.96%	1.0892	- 7.32%
PMB	111.5176	0	0.105588	0	5.1433	0	1.0194	0
KPMB	97.0756	+ 12.95%	0.141632	+ 34.14%	7.5815	+ 47.40%	1.0324	+ 1.28%
PPMB	140.4452	+ 25.89%	0.172107	+ 63.00%	6.2204	+ 20.94%	1.0360	+ 1.63%

**Table 3** The main functional groups of PSB, PPSB, and KPSB

PSB		PPSB		KPSB	
Wavenumbers (cm <sup>-1</sup> )	Assignment	Wavenumbers (cm <sup>-1</sup> )	Assignment	Wavenumbers (cm <sup>-1</sup> )	Assignment
3434.12	-OH	3438.94	-OH	3436.53	-OH
2923.56	Stretching C-H	2927.89	Stretching C-H	2927.41	Stretching C-H
1580.86	Ring C-C stretch of phenyl	1584.72	Ring C-C stretch of phenyl	1583.27	Ring C-C stretch of phenyl
1099.71	stretching vibrations of C-O	1099.71	Stretching PO <sub>2</sub> <sup>-</sup> symmetric (phosphate II)	1092.48	Stretching PO <sub>2</sub> <sup>-</sup> symmetric (phosphate II) v <sub>asym</sub> (C-O-C) (polysaccharides-cellulose)
581.91	C-H	586.25	C-H	579.51	C-H

**Table 4** The main functional groups of PMB, PPMB, and KPMB

PMB		PPMB		KPMB	
Wavenumbers (cm <sup>-1</sup> )	Assignment	Wavenumbers (cm <sup>-1</sup> )	Assignment	Wavenumbers (cm <sup>-1</sup> )	Assignment
3438.94	Stretching O–H asymmetric	3439.42	Stretching O–H asymmetric	3426.89	Stretching O–H asymmetric
2928.38	Stretching C–H	2931.75	C–H stretching bands $\nu_{as}$ CH <sub>2</sub>	1448.28	Asymmetric CH <sub>3</sub> bending of the methyl groups of proteins
1620.39	Ring C–C stretch of phenyl	1619.91	Ring C–C stretch of phenyl	1038.48	Ring stretching vibrations mixed strongly with CH in-plane bending
1414.53	Stretching C–N, deformation N–H, deformation C–H	1095.85	Stretching PO <sub>2</sub> <sup>-</sup> symmetric	872.15	C3' <i>endo/anti</i> (A-form helix) conformation
1049.08	Ring stretching vibrations mixed strongly with	564.56	C–H	566.97	C–H
596.86	CH out-of-plane bending vibrations				
562.63	C–H				

consistent with the higher specific surface area of acid-treated biochars (refer to Table 2). The pore diameters of these six biochars are mainly in the range of 2–15 nm, which are typical mesoporous materials. The pore size of these six biochar is relatively dense (i.e., 2 and 10 nm). The maximum pore size is between 4.89 and 5.09 nm (refer to Fig. 5). Water molecules have a diameter of 0.4 nm. This facilitates the diffusion and adsorption of water molecules.

Figure 6 shows the XRD patterns that are useful to interpret crystalline phases of six different biochars. A sharp diffraction peak (101 crystal plane) appears at  $2\theta = 26.5^\circ$ , which was detected as SiO<sub>2</sub> (refer to Fig. 6a). After modification, the minerals of pristine biochar were similar to H<sub>3</sub>PO<sub>4</sub>-modified biochar, which indicates that the crystal structure underwent little variation. H<sub>3</sub>PO<sub>4</sub> modification caused slight changes in XRD due to reactions with carbonaceous components. As expected, amorphous carbon peaks of PSB, KPSB, and PPSB are found. Figure 6b indicates the presence of KCl, K<sub>2</sub>O, and C<sub>6</sub>H<sub>4</sub>O<sub>4</sub> in PMB, the existence of CaCO<sub>3</sub>, K<sub>2</sub>O, and KO<sub>2</sub> in KPMB, and SiO<sub>2</sub>, CaCO<sub>3</sub>, and C in PPMB. With a gradual increase in temperature, carbonaceous components reacted with KOH and formed K<sub>2</sub>CO<sub>3</sub>. K<sub>2</sub>O and KO<sub>2</sub> were converted to the K<sub>2</sub>CO<sub>3</sub> when the temperature was raised at 700 °C [17]. The components in pig manure biochar have undergone a significant change upon modification. However, the existence of potassium in pristine biochar is likely to interfere with the mechanism involving KOH modification. Therefore, further elemental tracking studies are needed to understand this mechanism.

### 3.2 Water retention behavior of six biochars in soil improvement

The water retention characteristics of the samples are shown in Fig. 7. As compared with bare soil, the addition of biochar

shows a significant increase in water retention. In particular, the sample with 5% biochar content significantly improved the water retention capacity of the soil. With an addition of H<sub>3</sub>PO<sub>4</sub>-modified biochar, the soil's ability to retain water gradually increases, which is consistent with the results of other related studies [41]. The water improving ability of water containing can be attributed to three reasons. The addition of fine biochar particles to relatively coarse soil particles reduces average pore size, which helps to maintain moisture through capillary action [42]. Secondly, the existence of pores within the biochar particles also enables additional storage in a single biochar particle matrix (refer to Fig. 2). Thirdly, the presence of hydrophilic surface bonds (mainly hydroxyl (OH)) further helps to improve the retention capacity of the soil-biochar composite material (refer to Fig. 3) [43]. As observed from Fig. 7, generally, it can be observed that variation of water content in most of the samples follows a similar trend under drying-wetting cycles. The first drying stage has the greatest impact. In the first drying stage, the moisture content of all samples changed more significantly than in the later drying stage. The retention of water content of all samples in the first drying cycle was higher than that in the second cycle. As compared with the difference in moisture content among samples at the end of the dry cycle, the moisture content at the end of the wet cycle has a greater difference. The water retained in the sample decreases during the dry period and increases during the wet period [44].

In order to interpret the influence of various biochars on soil water retention and cracking, Fig. 8 was plotted by considering critical points (maximum water content and CIF during dry–wet cycles) from Fig. 7. As observed from Fig. 8, 2% dosage of biochar amended soil did not significantly increase the maximum water content as compared with bare soil (BS), while 5% and 8% biochar content presented



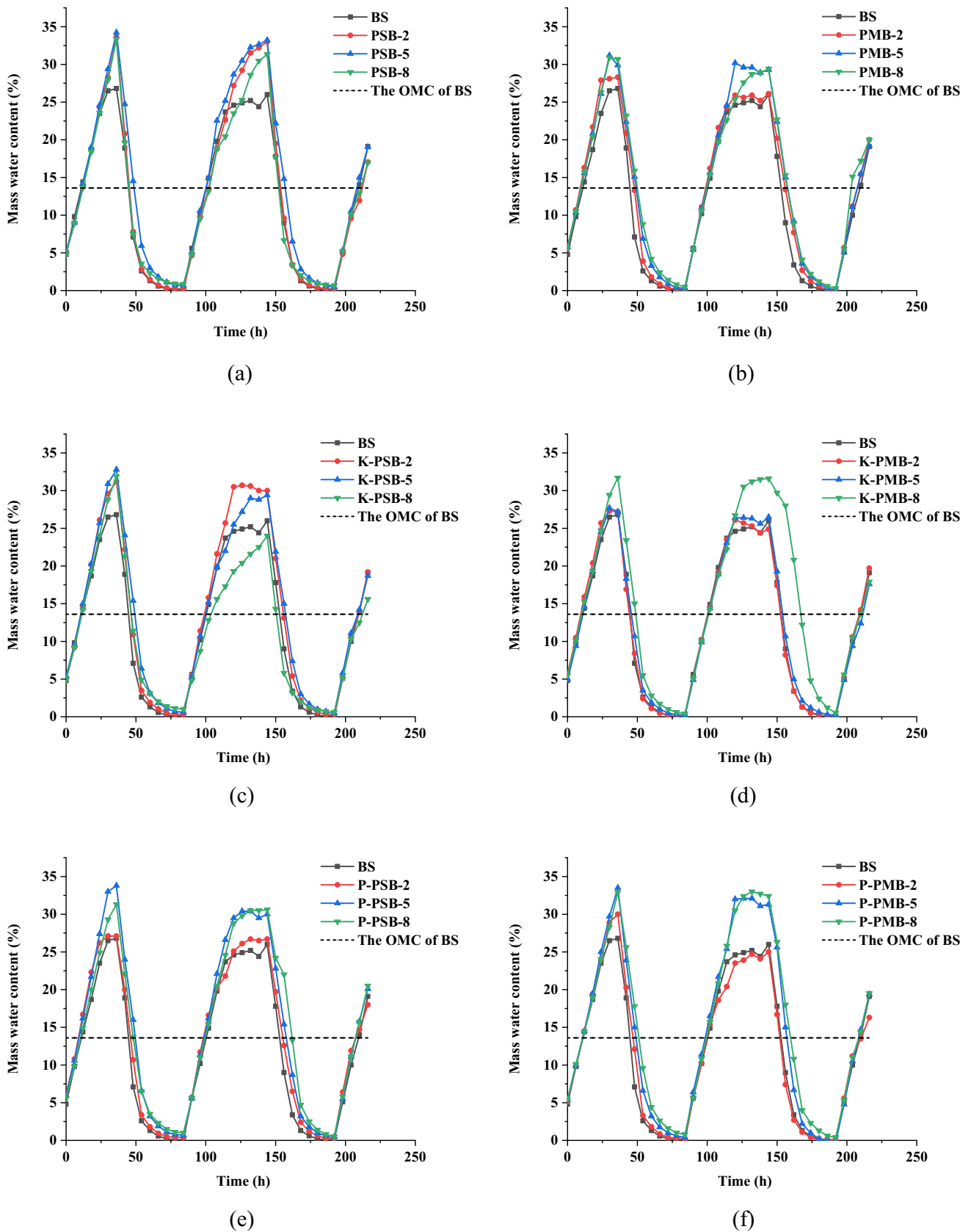


**Fig. 7** Gravimetric water content of biochar amended soil samples with different biochar contents for **a** PSB, **b** PMB, **c** KPSB, **d** KPMB, **e** PPSB, and **f** PPMB

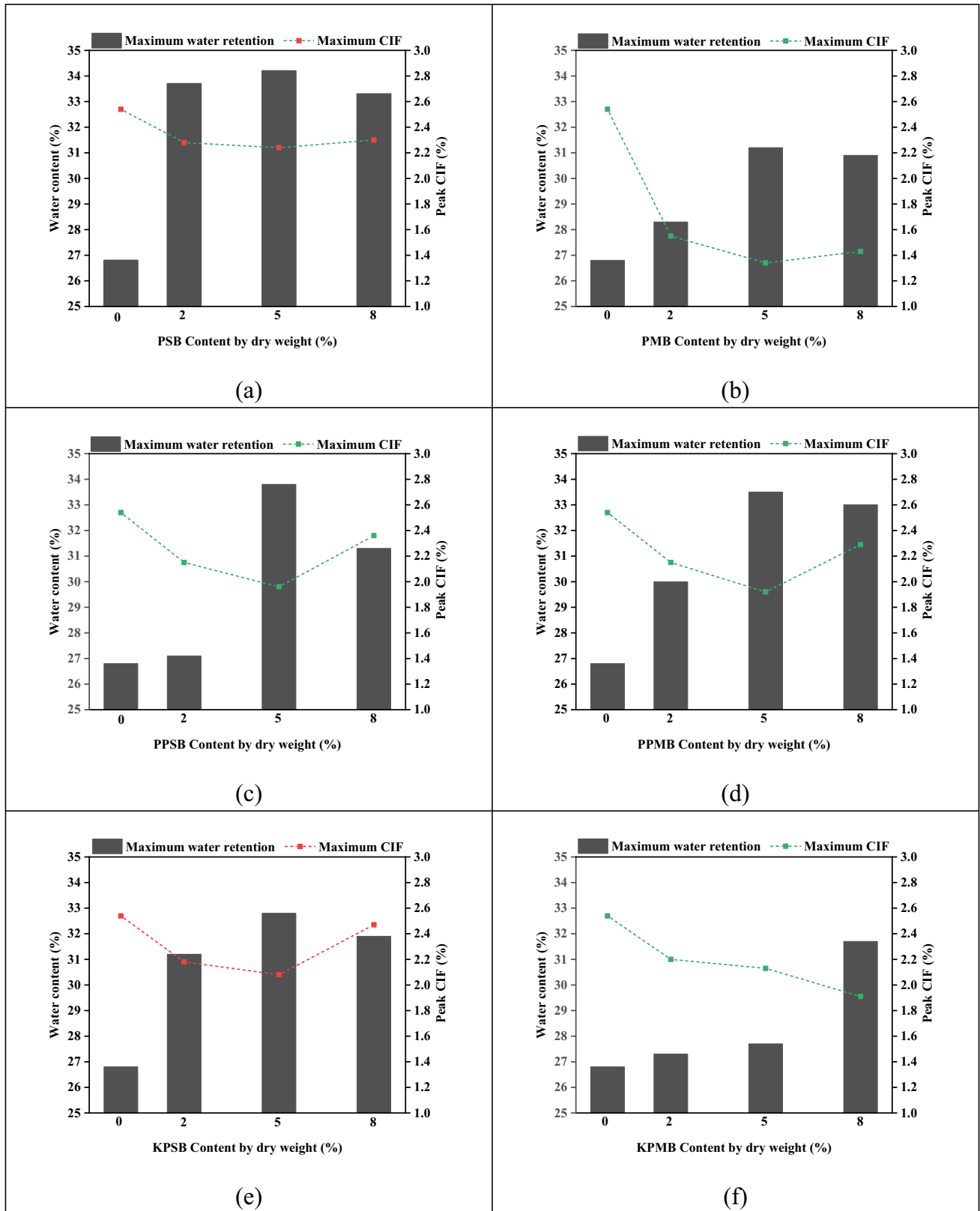


**Fig. 8** Variation of maximum water retention and peak CIF with biochar content for **a** PSB, **b** PMB, **c** PPSB, **d** PPMB, **e** KPSB, and **f** KPMB

a noticeable increment in the peak water content. The water retention capacity of soil samples with a combined amount of 2–8% of KOH modified biochar is better than BS. It can be also observed that the water retention of biochars was not directly related to surface area (refer to Table 2). In general, plant-based peach shell biochars retained higher water content as compared to animal-based pig manure biochar. This is despite the higher surface area of PMBs as compared to PSBs (Table 2). This trend of water retention is likely due to ligno-cellulosic nature of plant-based biochars, which are able to attract more water than animal-based biochars. It is consistent with the literature [31]. KOH-treated biochar generally reduces water retention due to its lower surface area (Table 2). Further, it is also found that for PSBs, there is an optimal content of 5%, at which water retention is maximum. The water retained in PSB-8 is lower than that of PSB-5, which may be due to excess fine particles. On the other hand, for PMB, the optimal water content is not conclusive. An appropriate amount of biochar can fill soil voids, reduce evaporation rate, and increase soil and water conservation capacity [45]. It can be concluded that functional groups as well as surface area are important parameters affecting water retention among modified biochars.

### 3.3 Discussion on cracking behavior with water retention and biochar content

Maximum CIF in all samples shows opposite trend to that of maximum water content (Fig. 8). The maximum CIF generally decrease with an increase in biochar content. At 5% biochar content, the value of CIF tends to become minimum. This is consistent with the previous study [46–48]. It is expected that the biochar particles influenced the interlocking and cohesive characteristics of soil through surface functional groups [46]. The increase of water content can reduce the stress and crack formation in soil [49]. Interestingly, there is a slight increase in CIF beyond that. It is hypothesized that excess superfluous dosage of biochar particles might float around the soil resulting in a less rigid matrix system [48], which may ultimately cause less resistance to crack propagation. Therefore, an appropriate dosage of biochar with soil might generate better effects in the crack suppression.

Among all biochars (Fig. 8), soil amended with PMB is found to possess the lowest CIF value. Lower CIF occurs in soil amended with PMB at dosage of around 8%. This is despite lower water retention ability of PMB as compared to PSBs. Possible reason could be due to higher roughness and shape of PMB biochar particles [47] that increases the friction in soil and limits the crack formation and shrinkage of biochar amended soil. Further studies are needed to explore the mechanism of crack suppression in soils amended with different types of biochars. The difference in

crack suppression ability between unmodified biochar and modified biochar is due to the change in pore volume and functionality caused by chemical treatment. For plant-based peach shell biochar, 5% dosage of biochar always has smaller CIF value as compared with other dosages. At 5% dosage, soils modified with  $H_3PO_4$ -treated biochars are found to suppress crack more than those modified with KOH-treated biochars. Soil amended with PPSB-5 shows lower CIF values than those of PSB-5 and KPSB-5, respectively. This outcome was consistent with the variation in specific area and functional groups. The improvement in the specific area of KOH-modified biochar is lower than  $H_3PO_4$ -modified biochar. In addition, KOH modification generated non-hydrophilic groups (ring C–C and -CH<sub>3</sub>).

Based on the above results, one can summarize that modified plant-based biochar (PPSB, KPSB) has greater performance in crack suppression than pristine peach shell biochars (PSB) while pristine animal-based biochar (PMB) shows better performance in crack suppression than modified biochar (PPMB, KPMB). Chemically modified different biochars show different results in water retention and crack suppression. The result reminds that if it is aimed to improve the water retention ability and crack suppression of soil that the modification by  $H_3PO_4$  and KOH needs to consider the types of biochar.

## 4 Conclusion

This study investigates the soil cracking and water retention behavior under influence of KOH- and  $H_3PO_4$ -modified peach shell and pig manure biochars. Micro-structural characterization of biochars with and without modification was done to analyze water retention and cracking. The performance of water retention in case of soils amended with plant-based PSB was generally greater than animal-based pig manure biochars and bare soil.  $H_3PO_4$ -modified biochar has been found to have much impact on soil water retention as compared to KOH-modified biochar.

Interestingly, there is no direct correlation between cracking and water retention. Pig manure biochar (PMB) can suppress cracking more than other chemically modified biochars. This may be due to resistance generated against tension due to angularity of pig manure biochar particles. The inhibition effect of biochars on soil cracks was basically the same after chemical modification. While the result of this study only represents the conditions under several dry–wet cycles with biochar, the mechanism of crack expansion influenced by modified biochar needs to be further studied. The effect of modified biochar on soil water retention and crack resistance is significantly different from that of pristine biochar. In this study, chemical modification enhanced the cracking resistance of plant-based PSB. On the other hand,

**Table 5** Comparison of peak CIF and maximum retained moisture content of biochar-amended soil between present study and literature

Reference	Soil type	Amendment	Peak CIF(%)	Max moisture content(%)
Bordoloi et al. [42]	Sand with fines	Bare soil	7.13	28.97 (V)
		2% biochar produced by water hyacinth	5.29	31.97 (V)
		5% biochar produced by water hyacinth	3.73	36.33 (V)
		10% biochar produced by water hyacinth	3.20	41.38 (V)
Wang et al. [50]	Expansive clay	Bare soil	11.95	55.12 (V)
		5% biochar produced by straw	7.92	56.66 (V)
		10% biochar produced by straw	6.08	59.77 (V)
		15% biochar produced by straw	6.30	60.28 (V)
Present study	Clayey sand	Bare soil	2.54	26.80 (V)
		2% biochar produced by peach shell biochar	2.28	33.70 (V)
		5% biochar produced by peach shell biochar	2.24	34.20 (V)
		8% biochar produced by peach shell biochar	2.30	33.30 (V)
		2% KOH modified peach shell biochar	2.18	31.20 (V)
		5% KOH modified peach shell biochar	2.08	32.80 (V)
		8% KOH modified peach shell biochar	2.47	31.90 (V)
		2% H <sub>3</sub> PO <sub>4</sub> modified peach shell biochar	2.15	27.10
		5% H <sub>3</sub> PO <sub>4</sub> modified peach shell biochar	1.96	33.80
		8% H <sub>3</sub> PO <sub>4</sub> modified peach shell biochar	2.36	31.30
		2% biochar produced by pig manure biochar	1.55	28.30
		5% biochar produced by pig manure biochar	1.34	31.20
		8% biochar produced by pig manure biochar	1.43	30.90
		2% KOH modified pig manure biochar	2.2	27.30
		5% KOH modified pig manure biochar	2.13	27.70
		8% KOH modified pig manure biochar	1.91	31.70
2% H <sub>3</sub> PO <sub>4</sub> modified pig manure biochar	2.15	30.00		
5% H <sub>3</sub> PO <sub>4</sub> modified pig manure biochar	1.92	33.50		
8% H <sub>3</sub> PO <sub>4</sub> modified pig manure biochar	2.29	33.00		

\*V represents volumetric water content; Moisture content represent gravimetric water content

the cracking resistance of animal-based PMB is higher or similar than original biochars for some scenarios. In most cases, 5–8% biochar content can be considered an optimal range for inhibiting soil cracks and improvement in water retention. In this study, the CIF obtained by adding 5% PMB to the soil was only 1.92%. It is significantly smaller than the CIF values obtained in other studies (refer to Table 5 [42, 50]).

It is also possible to combine biochar with other methods to improve the performance of WRC and CIF, such as microbial CaCO<sub>3</sub> precipitation technology (MICP). The modified biochar can play a role as media to provide attachment sites for bacteria, which may effectively enhance bacterial activity. Modified biochar also can be utilized as a kind of nanocomposite materials studying its improvement of electrical properties, thermal conductivity, and functionality [51]. The innovation of this experiment is to explore the effect of chemically modified biochar on soil water retention and inhibition of soil cracking and obtain the valid experimental result. However, this study did not consider the effect of biochar particle size on soil moisture content and inhibition of soil cracking,

which requires further attention. Additionally, it should be noted that the results are based on given testing conditions and hence cannot be generalized for other soil types and testing boundary conditions. More studies are needed to evaluate the influence of various biochar types produced under different pyrolysis conditions [52] on water retention and cracking in soils of varying grain size distribution.

**Author contribution** First author has made significant contribution in writing draft and revising manuscript and analyses. Second, third, and fourth authors have helped in setting up of experiment, data collection, and plotting of graphs. Fifth, sixth, and seventh authors have done chemical modification of biochar using acid and base and also help in revising manuscript. Eighth author helped in providing overall planning, supervision, allocation of resources, and also in developing initial idea for research. Ninth author has helped in co-supervision, providing comments, and editing of manuscript.

**Funding** The authors are thankful to National Natural Science Foundation (NSFC) for project grant (No. 41907252) for the support.

**Data availability** The data can be made available upon request.

## Declarations

**Conflict of interest** The authors declare no competing interests.

## References

- Tang CS, Shi B, Cui YJ, Liu C, Gu K (2012) Desiccation cracking behavior of polypropylene fiber–reinforced clayey soil. *Can GeotechEOTECH J* 49:1088–1101. <https://doi.org/10.1139/2012-067>
- DeCarlo KF, Caylor KK (2019) Biophysical effects on soil crack morphology in a faunally active dryland vertisol. *Geoderma* 334:134–145. <https://doi.org/10.1016/j.geoderma.2018.07.042>
- Preston S, Wirth S, Ritz K, Griffiths BS, Young IM (2001) The role played by microorganisms in the biogenesis of soil cracks: importance of substrate quantity and quality. *Soil Biol Biochem* 33:1851–1858. [https://doi.org/10.1016/S0038-0717\(01\)00113-4](https://doi.org/10.1016/S0038-0717(01)00113-4)
- Kalkan E (2009) Influence of silica fume on the desiccation cracks of compacted clayey soils. *Appl Clay Sci* 43:296–302. <https://doi.org/10.1016/j.clay.2008.09.002>
- Liu J, Ganesan SP, Li X, Garg A, Singhal A, Dosetti KD, Feng H (2020) Dynamics of biochar-silty clay interaction using in-house fabricated cyclic loading apparatus: a case study of coastal clay and Novel Peach Biochar from the Qingdao Region of China. *Sustainability-Basel* 12:2599. <https://doi.org/10.3390/su12072599>
- Tang C, Shi B, Liu C, Zhao L, Wang B, Tang C, Shi B, Liu C, Zhao L, Wang B (2008) Influencing factors of geometrical structure of surface shrinkage cracks in clayey soils. *Eng Geol* 101:204–217. <https://doi.org/10.1016/j.enggeo.2008.05.005>
- Yu OY, Raichle B, Sink S (2013) Impact of biochar on the water holding capacity of loamy sand soil. *Int J Energy Envir E* 4:1–9. <https://doi.org/10.1186/2251-6832-4-44>
- Garg A, Huang H, Kushvaha V, Madhushri P, Kamchoom V, Wani I, Zhu HH (2020) Mechanism of biochar soil pore–gas–water interaction: gas properties of biochar-amended sandy soil at different degrees of compaction using KNN modeling. *Acta Geophys* 68:207–217. <https://doi.org/10.1007/s11600-019-00387-y>
- Abrol, V., Ben-Hur, M., Verheijen, F. G., Keizer, J. J., Martins, M. A., Tenaw, H., ... & Graber, E. R. (2016). Biochar effects on soil water infiltration and erosion under seal formation conditions: rainfall simulation experiment. *J Soil Sediment*, 16:2709–2719. <https://doi.org/10.1007/s11368-016-1448-8>
- Barnes RT, Gallagher ME, Masiello CA, Liu Z, Dugan B (2014) Biochar-induced changes in soil hydraulic conductivity and dissolved nutrient fluxes constrained by laboratory experiments. *PLoS ONE* 9:e108340. <https://doi.org/10.1371/journal.pone.0108340>
- Sun F, Lu S (2014) Biochars improve aggregate stability, water retention, and pore-space properties of clayey soil. *J Plant Nutr Soil Sc* 177:26–33. <https://doi.org/10.1002/jpln.201200639>
- Yoshizawa S (2016) Biochar for carbon storage in the soil and for soil improvement. *Carbon* 100:263. <https://doi.org/10.1016/2Fj.carbon.2015.12.018>
- Bharath KN, Madhu P, Gowda TY, Sanjay MR, Kushvaha V, Siengchin S (2020) Alkaline effect on characterization of discarded waste of Moringa oleifera fiber as a potential eco-friendly reinforcement for biocomposites. *J Polym Environ* 28:2823–2836. <https://doi.org/10.1007/s10924-020-01818-4>
- Wani I, Sharma A, Kushvaha V et al (2020) Effect of pH, volatile content, and pyrolysis conditions on surface area and O/C and H/C ratios of biochar: towards understanding performance of biochar using simplified approach. *J Hazard Toxic Radio* 24:04020048. [https://doi.org/10.1061/\(ASCE\)HZ.2153-5515.0000545](https://doi.org/10.1061/(ASCE)HZ.2153-5515.0000545)
- Cheng, N., Wang, B., Wu, P., Lee, X., Xing, Y., Chen, M., & Gao, B (2021) Adsorption of emerging contaminants from water and wastewater by modified biochar: a review. *Environ Pollut* 116448. <https://doi.org/10.1016/j.envpol.2021.116448>.
- Wani, I., Ramola, S., Garg, A., & Kushvaha, V. (2021). Critical review of biochar applications in geoenvironmental infrastructure: moving beyond agricultural and environmental perspectives. *Biomass Convers and Bior*, 1-29. <https://doi.org/10.1007/s13399-021-01346-8>
- Liu L, Li Y, Fan S (2019) Preparation of KOH and H3PO4 modified biochar and its application in methylene blue removal from aqueous solution. *Processes* 7:891. <https://doi.org/10.3390/pr7120891>
- Ding Z, Hu X, Wan Y, Wang S, Gao B (2016) Removal of lead, copper, cadmium, zinc, and nickel from aqueous solutions by alkali-modified biochar: Batch and column tests. *J Ind Eng Chem* 33:239–245. <https://doi.org/10.1016/j.jiec.2015.10.007>
- Mohan D, Sarswat A, Ok YS, Pittman CU Jr (2014) Organic and inorganic contaminants removal from water with biochar, a renewable, low cost and sustainable adsorbent—a critical review. *Biore-source Technol* 160:191–202. <https://doi.org/10.1016/j.biortech.2014.01.120>
- Inyang, M. I., Gao, B., Yao, Y., Xue, Y., Zimmerman, A., Mosa, A., ... & Cao, X. (2016). A review of biochar as a low-cost adsorbent for aqueous heavy metal removal. *Crit Rev Env Sci Tec*, 46(4), 406–433. <https://doi.org/10.1080/10643389.2015.1096880>
- Chen, J., Qiu, X., Fang, Z., Yang, M., Pokeung, T., Gu, F., ... & Lan, B. (2012). Removal mechanism of antibiotic metronidazole from aquatic solutions by using nanoscale zero-valent iron particles. *Chem Eng J*, 181, 113–119. <https://doi.org/10.1016/j.cej.2011.11.037>
- Fan Y, Wang B, Yuan S, Wu X, Chen J, Wang L (2010) Adsorptive removal of chloramphenicol from wastewater by NaOH modified bamboo charcoal. *Biore-source Technol* 101:7661–7664. <https://doi.org/10.1016/j.biortech.2010.04.046>
- Jing XR, Wang YY, Liu WJ, Wang YK, Jiang H (2014) Enhanced adsorption performance of tetracycline in aqueous solutions by methanol-modified biochar. *Chem Eng J* 248:168–174. <https://doi.org/10.1016/j.cej.2014.03.006>
- Liang, J., Li, X., Yu, Z., Zeng, G., Luo, Y., Jiang, L., ... & Wu, H. (2017). Amorphous MnO2 modified biochar derived from aerobically composted swine manure for adsorption of Pb (II) and Cd (II). *ACS Sustain Chem Eng*, 5 5049–5058. <https://doi.org/10.1021/acssuschemeng.7b00434>
- Sadegh-Zadeh F, Seh-Bardan BJ (2013) Adsorption of As (III) and As (V) by Fe coated biochars and biochars produced from empty fruit bunch and rice husk. *J Environ Chem Eng* 1:981–988. <https://doi.org/10.1016/j.jece.2013.08.009>
- Yin Q, Wang R, Zhao Z (2018) Application of Mg–Al-modified biochar for simultaneous removal of ammonium, nitrate, and phosphate from eutrophic water. *J Clean Prod* 176:230–240. <https://doi.org/10.1016/j.jclepro.2017.12.117>
- Zhao L, Zheng W, Mašek O, Chen X, Gu B, Sharma BK, Cao X (2017) Roles of phosphoric acid in biochar formation: synchronously improving carbon retention and sorption capacity. *J Environ Qual* 46:393–401. <https://doi.org/10.2134/jeq2016.09.0344>
- Wang J, Kaskel S (2012) KOH activation of carbon-based materials for energy storage. *J Mater Chem* 22:23710–23725. <https://doi.org/10.1039/C2JM34066F>
- ASTM Committee D-18 on Soil and Rock. (2017) Standard practice for classification of soils for engineering purposes (Unified Soil Classification System) I. ASTM International.
- Huang, H., Cai, W. L., Zheng, Q., Chen, P. N., Huang, C. R., Zeng, Q. J., ... & Kushvaha, V. (2020, March). Gas permeability in soil amended with biochar at different compaction states. In

- IOP Conference Series: Carpath J Earth Env (Vol. 463, No. 1, p. 012073). IOP Publishing. <https://doi.org/10.1088/1755-1315/463/1/012073>
31. Mei, G., Kumar, H., Huang, H., Cai, W., Reddy, N. G., Chen, P., ... & Ganeshan, S. P. (2021) Desiccation cracks mitigation using biomass derived carbon produced from aquatic species in South China Sea. *Waste Biomass Valori* 12:1493-1505 <https://doi.org/10.1007/s12649-020-01057-7>
  32. Bordoloi S, Gopal P, Boddu R, Wang Q, Cheng YF, Garg A, Sreedeeep S (2019) Soil-biochar-water interactions: role of biochar from *Eichhornia crassipes* in influencing crack propagation and suction in unsaturated soils. *J Clean Prod* 210:847–859. <https://doi.org/10.1016/j.jclepro.2018.11.051>
  33. Ma K, Conrad R, Lu Y (2012) Responses of methanogen *mcrA* genes and their transcripts to an alternate dry/wet cycle of paddy field soil. *Appl Environ Microb* 78:445–454. <https://doi.org/10.1128/AEM.06934-11>
  34. Gopal, P., Bordoloi, S., Ratnam, R., Lin, P., Cai, W., Buragohain, P., ... & Sreedeeep, S. (2019) Investigation of infiltration rate for soil-biochar composites of water hyacinth. *Acta Geopuys* 67: 231-246 <https://doi.org/10.1007/s11600-018-0237-8>
  35. Li Y, Ling X, Su L, An L, Li P, Zhao Y (2018) Tensile strength of fiber reinforced soil under freeze-thaw condition. *Cold Reg Sci Technol* 146:53–59. <https://doi.org/10.1016/j.coldregions.2017.11.010>
  36. Song C, Zheng H, Shan S, Wu S, Wang H, Christie P (2019) Low-temperature hydrothermal carbonization of fresh pig manure: effects of temperature on characteristics of hydrochars. *J Environ Eng-Asce* 145:04019029. [https://doi.org/10.1061/\(ASCE\)EE.1943-7870.0001475](https://doi.org/10.1061/(ASCE)EE.1943-7870.0001475)
  37. Qing-yu L, Min-zheng S, Li-lan D, Qin D, Yong-zhu L. (2007) Comparison of FT-IR spectrum of *Selaginella involvens* Spring. *Journal of Yunnan Normal University (Natural Sciences Edition)* 03
  38. Calvete T, Lima EC, Cardoso NF, Dias SL, Ribeiro ES (2010) Removal of brilliant green dye from aqueous solutions using home made activated carbons. *Clean-Soil Air Water* 38:521–532. <https://doi.org/10.1002/clen.201000027>
  39. Sahin O, Taskin MB, Kaya EC, Atakol O, Emir E, Inal A, Gunes A (2017) Effect of acid modification of biochar on nutrient availability and maize growth in a calcareous soil. *Soil Use Manage* 33:447–456. <https://doi.org/10.1111/sum.12360>
  40. Thommes M, Kaneko K, Neimark AV, Olivier JP, Rodriguez-Reinoso F, Rouquerol J, Sing KS (2015) Physisorption of gases, with special reference to the evaluation of surface area and pore size distribution (IUPAC Technical Report). *Pure Appl Chem* 87:1051–1069. <https://doi.org/10.1515/pac-2014-1117>
  41. Ni JJ, Chen XW, Ng CWW, Guo HW (2018) Effects of biochar on water retention and matric suction of vegetated soil. *Geotech Lett* 8:124–129. <https://doi.org/10.1680/jgele.17.00180>
  42. Bordoloi S, Garg A, Sreedeeep S, Lin P, Mei G (2018) Investigation of cracking and water availability of soil-biochar composite synthesized from invasive weed water hyacinth. *Bioresource Technol* 263:665–677. <https://doi.org/10.1016/j.biortech.2018.05.011>
  43. Gray M, Johnson MG, Dragila MI, Kleber M (2014) Water uptake in biochars: the roles of porosity and hydrophobicity. *Biomass Bioenerg* 61:196–205. <https://doi.org/10.1016/j.biombioe.2013.12.010>
  44. Brantley KE, Brye KR, Savin MC, Longer DE (2015) Biochar source and application rate effects on soil water retention determined using wetting curves. *Open J Soil Sci* 5:1. <https://doi.org/10.4236/ojss.2015.51001>
  45. Yang B, Li D, Yuan S, Jin L (2021) Role of biochar from corn straw in influencing crack propagation and evaporation in sodic soils. *CATENA* 204:105457. <https://doi.org/10.1016/j.catena.2021.105457>
  46. Jyoti Bora, M., Bordoloi, S., Kumar, H., Gogoi, N., Zhu, H. H., Sarmah, A. K., ... & Mei, G. (2021). Influence of biochar from animal and plant origin on the compressive strength characteristics of degraded landfill surface soils. *Int J Damage Mech* 30:484-501 <https://doi.org/10.1177/1056789520925524>
  47. Kumar H, Cai W, Lai J, Chen P, Ganesan SP, Bordoloi S, Mei G (2020) Influence of in-house produced biochars on cracks and retained water during drying-wetting cycles: comparison between conventional plant, animal, and nano-biochars. *J Soil Sediment* 20:1983–1996
  48. Ajayi AE, Rainer HORN (2017) Biochar-induced changes in soil resilience: effects of soil texture and biochar dosage. *Pedosphere* 27:236–247. [https://doi.org/10.1016/S1002-0160\(17\)60313-8](https://doi.org/10.1016/S1002-0160(17)60313-8)
  49. Kodikara, J. K., Barbour, S. L., & Fredlund, D. G. (2020) Desiccation cracking of soil layers. In *Unsaturated soils for Asia* (pp. 693–698). CRC Press.
  50. Wang H, Zhang K, Gan L, Liu J, Mei G (2021) Expansive soil-biochar-root-water-bacteria interaction: Investigation on crack development, water management and plant growth in green infrastructure. *Int J damage Mech* 30:595–617. <https://doi.org/10.1177/2F1056789520974416>
  51. Hemath M, MavinkereRangappa S, Kushvaha V, Dhakal HN, Siengchin S (2020) A comprehensive review on mechanical, electromagnetic radiation shielding, and thermal conductivity of fibers/inorganic fillers reinforced hybrid polymer composites. *Polym Composite* 41:3940–3965. <https://doi.org/10.1002/pc.25703>
  52. Huang H, Reddy NG, Huang X, Chen P, Wang P, Zhang Y, Huang Y, Lin P, Garg A (2021) Effects of pyrolysis temperature, feed-stock type and compaction on water retention of biochar amended soil. *Sci Rep* 11(1):1–19

**Publisher's Note** Springer Nature remains neutral with regard to jurisdictional claims in published maps and institutional affiliations.